Journal of Materials Chemistry C

Accepted Manuscript

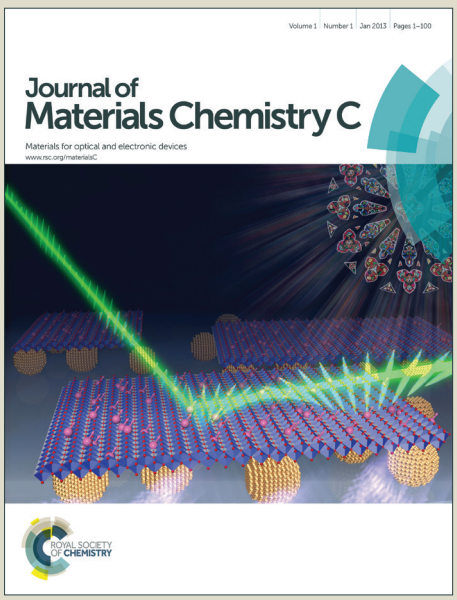

ROYAL SOCIETY OF CHEMISTRY

www.rsc.org/materialsC

Effect of Nb and Ta Substitution on Donor Electron Transport and Ultrafast Carrier Dynamics in Anatase TiO_2 Thin Films

Kalon Gopinadhan[1,4,*], Brijesh Kumar[1], Natalie Palina[5], M. Motapathula[1], I. Pallecchi[6], T. P. Sarkar[1,2], Y. Zhihua[1], J. Q. Chen[1], A. Annadi[1,2], A. Rana[1], Amar Srivastava[1,2], D. Marré[6], Jingsheng CHEN[1,4], Ariando[1,2], S. Dhar[1,7], A. Rusydi[1,2,5] and T. Venkatesan[1,3,4,*]

[1]NUSNNI-NanoCore, National University of Singapore, Singapore 117576

[2]Department of Physics, National University of Singapore, Singapore 117542

[3]Department of Electrical and Computer Engineering, National University of Singapore, Singapore 117576

[4]Department of Materials Science and Engineering, National University of Singapore, Singapore 117575, Singapore

[5]Singapore Synchrotron Light Source, National University of Singapore, Singapore 117603, Singapore

[6]CNR-SPIN and Università di Genova, Dipartimento di Fisica via Dodecaneso 33, Genova Italy 16146

[7]Department of Physics, Shiv Nadar University UP, India 201314

E-mail: gopinadhan@iitkalumni.org (KG);eletv@nus.edu.sg (TV)

Keywords: anatase TiO_2, Polarons, Femtosecond carrier dynamics, photovoltaics, electrical transport

ABSTRACT

Ta and Nb substituted TiO_2 is an important transparent conducting oxide which has potential for applications in photo-voltaics, photocatalysis, water splitting/CO_2 sequestration. Besides donating electrons what are the effects of Nb and Ta substitution? Here we observe strong experimental evidence of Ta and Nb substitution induced large and small polarons in anatase TiO_2 epitaxial thin films. The degenerate donor electrons (from both Nb and Ta) show a high temperature T^3 dependence of electrical resistivity confirming the presence of large polarons along with room temperature metallic transport. This is further confirmed by the enhancement in the

electron effective mass estimated from thermopower measurements. Femtosecond transient absorption (fs-TA) reveals the life time of Ti-t_{2g} and e_g levels and the separation of these levels are consistent with X-ray absorption spectroscopy (XAS) measurement. In addition, fs-TA reveals the presence of small polarons with life time substantially > 1 ns arising from defect levels, a consequence of Ta and Nb substitution. X-ray photoelectron spectroscopy (XPS) provides the evidence of Ti^{3+} which may be identified as the defects responsible for the small polarons. These long lived small polarons may provide a way to minimize recombination dynamics in TiO_2 based electrodes for photo-excited devices.

Introduction

Ta and Nb substituted TiO_2 is an important transparent conducting oxide which has potential for a wide range of applications.[1] The key parameter which determines the efficiency of these applications is the carrier life time. Therefore, in-depth understanding and manipulation of carrier life time of this material is of great importance for these applications. The important question is can we avoid recombination loss in TiO_2 electrodes? It is theoretically predicted that incorporating Ta and Nb into TiO_2 produces small polarons; a quasi-particle formed due to the interaction of electron and phonon, which forms a mid-gap level[2] and may reduce recombination loss. Large polarons on the other hand, are intermediate to free electrons and small polarons, which are expected to form energy levels very close the conduction band leading to metallic transport. There is a recent report of large polarons in single crystals of undoped anatase TiO_2 induced by oxygen vacancies,[3] but no such report exists for thin films of doped or undoped anatase TiO_2.

Being a wide band gap material with an energy gap of 3.2 eV, TiO_2 absorbs only 3-5% of the total solar radiation,[4] thus limiting the usage of this material in direct photovoltaic energy conversion applications. However, lowering the band gap or introducing mid-gap states will extend the absorption to visible range, which will increase the overall efficiency of photoconductive based devices. Disorder engineered TiO_2 known as black TiO_2 reduces the band gap,[5] where the disorder forms continuum levels with the conduction band and has been shown to increase the solar conversion efficiency. Defect induced mid-gap state absorption has also been demonstrated in rutile TiO_2 showing visible photochemical activity.[6] Thus, knowledge of the location of the mid-gap states and its lifetime in the Ta and Nb substituted TiO_2 would be an important step in our ability to manipulate these defect levels for the desired applications.

In this study, from electrical transport and femtosecond carrier dynamics, we show that Ta and Nb substitution influence electron transport and affect the photo-excited carrier dynamics via large and small polarons. We find a T^3 dependent metallic resistivity and an increase in effective mass as evidence for large polarons. fs-TA spectra show evidence for small polarons due to Ti^{3+}/Ti-vacancy states with a carrier life time longer than 1 ns. In addition, we find that the life time of t_{2g} and e_g is of the order of few ps.

Experimental Section

$Ti_{0.94}M_{0.06}O_2$ (M = Nb, Ta) thin films with a nominal thickness of 350 nm were grown by pulsed laser deposition (PLD) on $LaAlO_3$ (001) substrate at a temperature of 600±5 ^oC and at different oxygen partial pressures ($8x10^{-5}$ - $2x10^{-4}$ Torr). The PLD target was prepared by a solid-state reaction between 99.999% pure TiO_2 and Ta_2O_5 (Nb_2O_5) powders and the amount of Ta (Nb) in the deposited film was determined to be ~ 6 at.% by Rutherford backscattering spectrometry (RBS). At low thicknesses (~10 nm) the films are dominated by titanium

vacancy (V_{Ti}) which exhibit ferromagnetism [8] and at larger thicknesses (< 200 nm) the dominating defects lead to Kondo scattering but at higher thicknesses impurity scattering effects dominate. Higher film thickness (~350 nm) was selected to minimize magnetic effects on the electronic properties. The film thickness, composition and Ta/Nb substitution were accurately estimated by RBS/channeling. X-ray diffraction (XRD) data shows that the films are purely anatase TiO_2 with only (004) and (008) reflections (Figure S1). The ionic radii of Ti in the tetravalent state is 75.5 pm, whereas for Ta and Nb in the pentavalent state is 78 pm. Since both Ta and Nb are pentavalent and there is no difference in ionic radii, it is expected to have identical electrical properties. The larger ionic radii of Ta or Nb with respect to Ti leads to an expansion of the lattice upon doping as inferred from the XRD data (Figure S1). To determine the carrier concentration and mobility, a magnetic field (*H*) was applied normal to the film plane in the van der Pauw geometry (Al wire bonding) in a physical property measurement system (PPMS) equipped with a 9 T superconducting magnet. The magnetic field was swept from 1 to -1 T under a constant current. Thermoelectric properties characterization was performed in a PPMS system with the thermal transport option, in the temperature range of 10 to 300 K. Measurements were carried out in a slow temperature sweep (0.5 K/min), in high vacuum (10^{-6} Torr) and in magnetic field up to 9 T, applying a square-wave heat flow with adjustable period (from 400 s to 1450 s) and thermal gradient (from 0.1 K to few K). fs-TA experiments are carried out using a Ti:sapphire oscillator seeded amplifier laser system (Coherent-Libra Inc.). The amplifier gives an output with a central wavelength of 800 nm, pulse duration of 100 fs and a repetition rate of 1 kHz. The output beam is splitted into two portions. A large portion of the beam is used to pump a TOPAS-C (Light Conversion) that allows to tune the wavelength of the beam from 185 to 2200 nm. The other portion is focused at a sapphire plate to generate a white light continuum. The white light beam is splitted into two portions: one as a probe and another as a reference

to correct the pulse to pulse intensity fluctuations. Both the pump and probe beams are focused onto the same position of the samples. The delay between the pump and probe pulses are varied using a computer-controlled translation stage. Energy density of 80 $\mu J/cm^2$ was used to pump the samples.

Results and discussion

We first discuss the temperature dependent electrical properties of $Ti_{0.94}Ta_{0.06}O_2$ and $Ti_{0.94}Nb_{0.06}O_2$ anatase thin film samples. Figure 1(a) and (b) show the electrical resistivity of these samples grown at different oxygen partial pressures as a function of temperature from 300 to 2 K. The resistivity of all the samples shows metallic behavior up to a minimum resistivity point as the sample is cooled from 300 K. The resistivity shows an upturn with a semiconducting behavior below this temperature. Recently, Yamamoto *et al.*[7] discuss the difference in the nature of conductivity of anatase and rutile TiO_2 upon Nb and Ta substitution. They show by using screened hybrid density functional theory that the anatase phase of TiO_2 is metallic for both Nb and Ta doping due to hydrogen like donor state whereas the rutile phase is semiconducting for both Nb and Ta due to trapping of electrons at the Ti^{3+} states. While this study notices differences between Nb and Ta in the case of semiconducting rutile TiO_2, they do not see any significant differences in the anatase case which is in agreement with our results. Experimentally both Ta and Nb produce degenerate donors (carrier density is independent of temperature, Figure S2) which lead to metallic behavior. To understand the nature of the high temperature transport, different forms of electron- phonon scattering are considered. In a simple metallic three- dimensional system such as Cu, Pt, V, the temperature dependent electrical resistivity due to the interaction of electrons with acoustic phonons changes from T to T^5 below the Debye temperature (typically around 300 K).[8] However, for the Ta and Nb substituted TiO_2 (with Debye temperatures above 700 K), irrespective of the nature of the dopant, we see a clear T^3 dependence for temperatures above

the minimum resistivity point. This indicates a stronger interaction of electrons with phonons most likely a large polaron, a quasi-particle of electron and phonon. The large polaron is

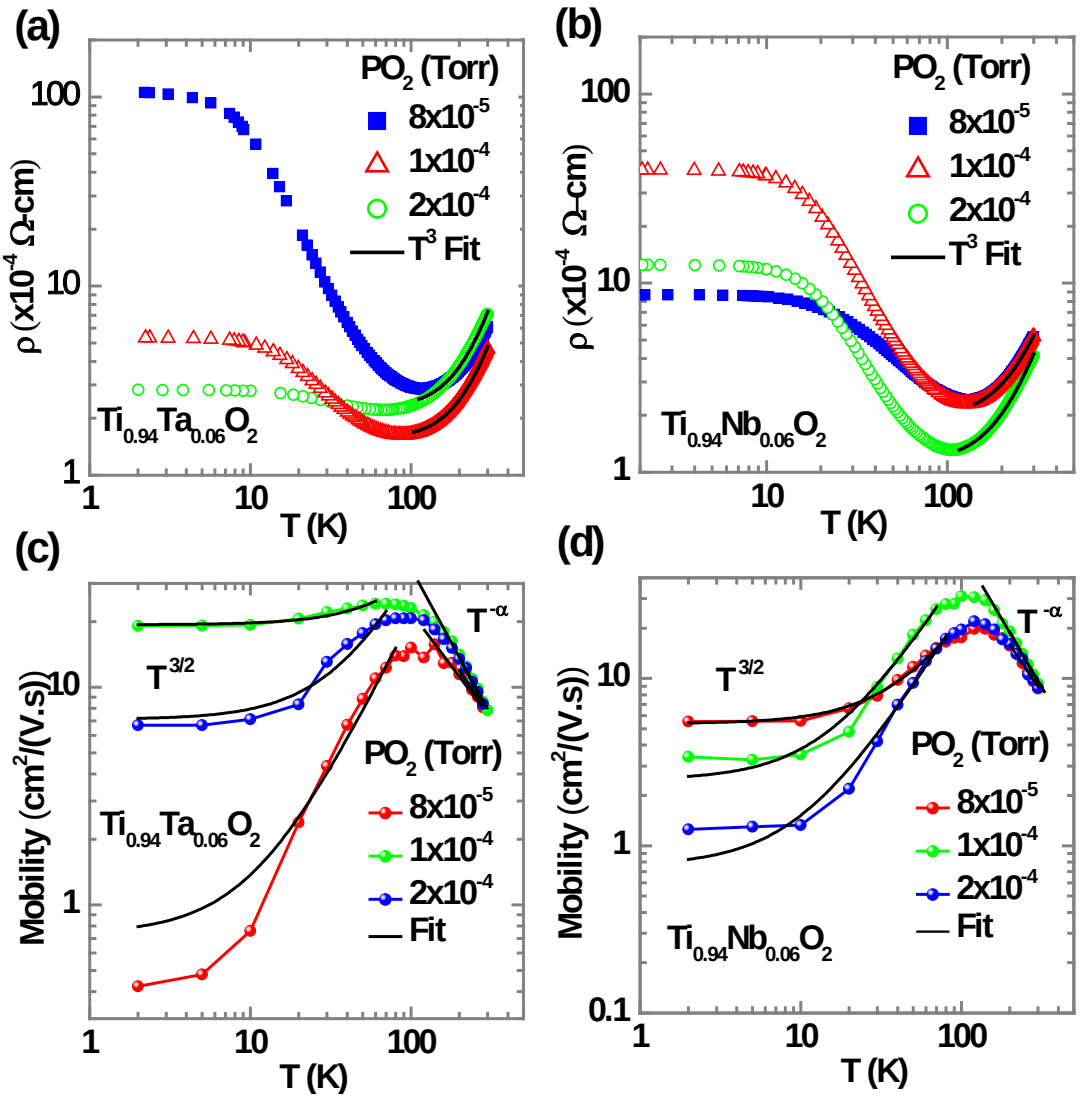

Fig. 1: (a) Resistivity (ρ) as a function of temperature (T) at different oxygen partial pressures for (a) $Ti_{0.94}Ta_{0.06}O_2$, and (b) $Ti_{0.94}Nb_{0.06}O_2$ thin films. In both cases above the resistivity minimum, ρ shows T^3 dependence which is typical of large polarons whereas the low temperature increase in resistivity is a result of ionized impurity scattering. Mobility (μ) as a function of temperature (T) at different oxygen partial pressures for (c) $Ti_{0.94}Ta_{0.06}O_2$, and (d) $Ti_{0.94}Nb_{0.06}O_2$ thin films. In both cases, above the maximum mobility point, the data is fitted by $T^{-\alpha}$ where α = 1.5 - 2.5. Below the mobility maximum, the curves are fitted by ionized impurity scattering term which is $T^{3/2}$.

supposed to have a higher effective mass than a free electron and we show evidence from thermopower measurements (Figure S3) that indeed the effective mass is enhanced due to interaction, which further confirms the formation of large polarons in Ta/Nb substituted TiO_2 samples.

To further establish the presence of large polarons, temperature dependent mobility measurement has been carried out. Figure 1(c) and (d) show the electron Hall mobility of $Ti_{0.94}Ta_{0.06}O_2$ and $Ti_{0.94}Nb_{0.06}O_2$ samples as a function of temperature from 300 to 2 K. These samples show a reasonable mobility of ~9 cm^2/V.s at 300 K which reaches a maximum of ~25 cm^2/V.s at low temperatures. The increase in mobility upon lowering the temperature implies a weakening of electron-phonon interaction in the sample which supports the description of large polarons. All the samples show a similar behavior in the temperature dependence of mobility with a maximum at low temperature. For temperatures above the maximum point, the mobility can be fitted by an electron-phonon coupling term ~$A*T^{-\alpha}$ with α varying from 1.5 - 2.5 and A is a constant which is found to depend on the sample preparation conditions and highly sensitive to the defect distribution. The mobility decreases for temperatures below the maximum mobility point despite the fact that electron-phonon interaction decreases as the temperature is lowered. Of many possibilities, ionized impurity scattering is the most plausible explanation for this enhanced scattering as the concentration of ionized donors (Ta^{5+} and Nb^{5+}) are very high ~ 6 at. % which should have a large scattering cross section at low temperatures. Ionized impurity scattering has been widely reported in extrinsic semiconductors such as Si, GaAs and InAs. Keeping this in mind, we have fitted our mobility results with $T^{3/2}$ dependence and an excellent agreement is seen. In addition, from thermopower measurements also, we see a change in effective mass with temperature signifying a change in the nature of the scattering, thus confirming the presence of ionized impurities in the system (Figure S4).

The chosen oxygen partial pressure (~10^{-4} Torr) was to minimize the oxygen vacancies in the samples. However, the variation of low temperature resistivity with oxygen pressure at first glance may suggest the presence of oxygen vacancies. A careful inspection of the room temperature resistivity among different samples suggests that the oxygen vacancies are not playing a significant role. At low temperatures, the oxygen vacancies will freeze out which means all the resistivity curves should be identical at low temperatures. However, we see a different behavior of resistivity at low temperatures which strongly suggests the minor role of oxygen vacancies in the sample. We attribute this to Ta/Nb substitution related defects such as Ti interstitials, Ti- vacancies, and Ti^{3+}. From the RBS channeling spectra (Figure S5), it is clear that in the case of $Ti_{0.94}Ta_{0.06}O_2$ sample prepared at PO_2 = 1x10^{-4} Torr, the minimum yield (χ) for Ti and Ta is 10 and 12% respectively and Ti substitutionality by Ta as 97.8%. The minimum yield of Ti is 10% which suggests that 10% Ti - ions are not in the crystal lattice means it could either be Ti-vacancies or Ti-interstitials. So the fine details of defects in the lattice have pronounced effect on the electrical resistivity since ionized impurity scattering dominates at low temperatures.

The carrier density of various films is provided in Figure S1. The Hall data is well described by a one-band model with no indication of any nonlinearity up to a maximum field of 9 T for all the film compositions. For 6 at. % Ta/Nb in TiO_2, assuming one electron per dopant should lead to an ideal carrier density of 1.75x10^{21} cm^{-3}. In our case the measured carrier density of 1.4 x10^{21} cm^{-3} suggests compensation by defects as the substitutionality of Ti with Ta/Nb is nearly perfect as measured by RBS channeling (Figure S5). These compensating defects (Ti^{3+} and V_{Ti}) are likely to appear inside the band gap of TiO_2 and our fs-TA measurements reported later show evidence for this.

The fs-TA spectra obtained from Ta substituted TiO_2 and Nb substituted TiO_2 thin films at different time delays by probing with a white light continuum after excitation with

the wavelength of 350 nm are shown in Figure 2a and 2b, respectively. A schematic representation of the energy levels involved in the transition of fs-TA spectra for both Ta and Nb case is shown in Figure 2c.The excitation of electrons from valence band to t_{2g} of the conduction band is marked as transition 'I' in this figure. The optical band gap of both Ta and Nb substituted TiO_2 film is estimated to be ~3.44 eV (Figure S6). Analysis based on the band structure of Ta and Nb substituted anatase TiO_2[1, 6] reveals many interesting features. A negative reflectivity feature is observed at ~2.17 eV which corresponds to the excited state absorption from Ti t_{2g} to e_g state of the 3d conduction band (transition 'II' in Figure 2c). It should be noted that the negative and positive reflectivity feature corresponds to absorption and emission respectively. Another transition with a positive reflectivity change appears at an energy ~2.13 eV in the TA spectra after ~15 ps, which has a lifetime longer than 1 ns (possibly much longer) and is attributed to the transition from mid-gap states to valence band (transition 'V' in Figure 2c). We believe that these mid-gap states could be formed due to large concentration of cationic defects in both the samples as evidenced from XPS and XAS spectra. These mid-gap states are absent in undoped anatase TiO_2 sample (Figure S7). Also, a small peak appears at ~1.95 eV of ~5 ps lifetime which corresponds to the radiative transition from e_g to t_{2g} (in agreement with the energy gap observed in these states from XAS measurement which we discuss later), suggesting a lifetime of 5 ps for the e_g state in the Nb substituted TiO_2 (transition 'III' in Figure 2c). No such feature is observed in the Ta-substituted TiO_2 film which could be due to non-radiative transition from e_g to t_{2g} or scattering loss of the carriers in the film. Transition 'IV' in Figure 2c represents the de-excitation of electrons from t_{2g} to mid-gap state, however we are not able to see this transition due to instrumental limitation. Further, kinetics of Ta substituted TiO_2 and Nb substituted TiO_2 thin films at a wavelength of 560 - 565 nm is shown in Figure 2d and e. The transient reflectivity spectra have been fitted with a two-exponential decay function:

$\Delta R/R = -A_1 \exp(-t/\tau_1) - A_2 \exp(-t/\tau_2)$ where A is the time independent coefficient and τ is the time constant. The fit gives two time constants for both Ta (2 and 15 ps) and Nb (1.7 and 10.4 ps) cases. This may imply the appearance of two different optical phonon life times as a result of Ta/Nb substitution in TiO_2 which induces resonant states in the t_{2g} levels.[2] The possibility of hot electron injection is ruled out as its typical life time is expected to be of the order of femtosecond.

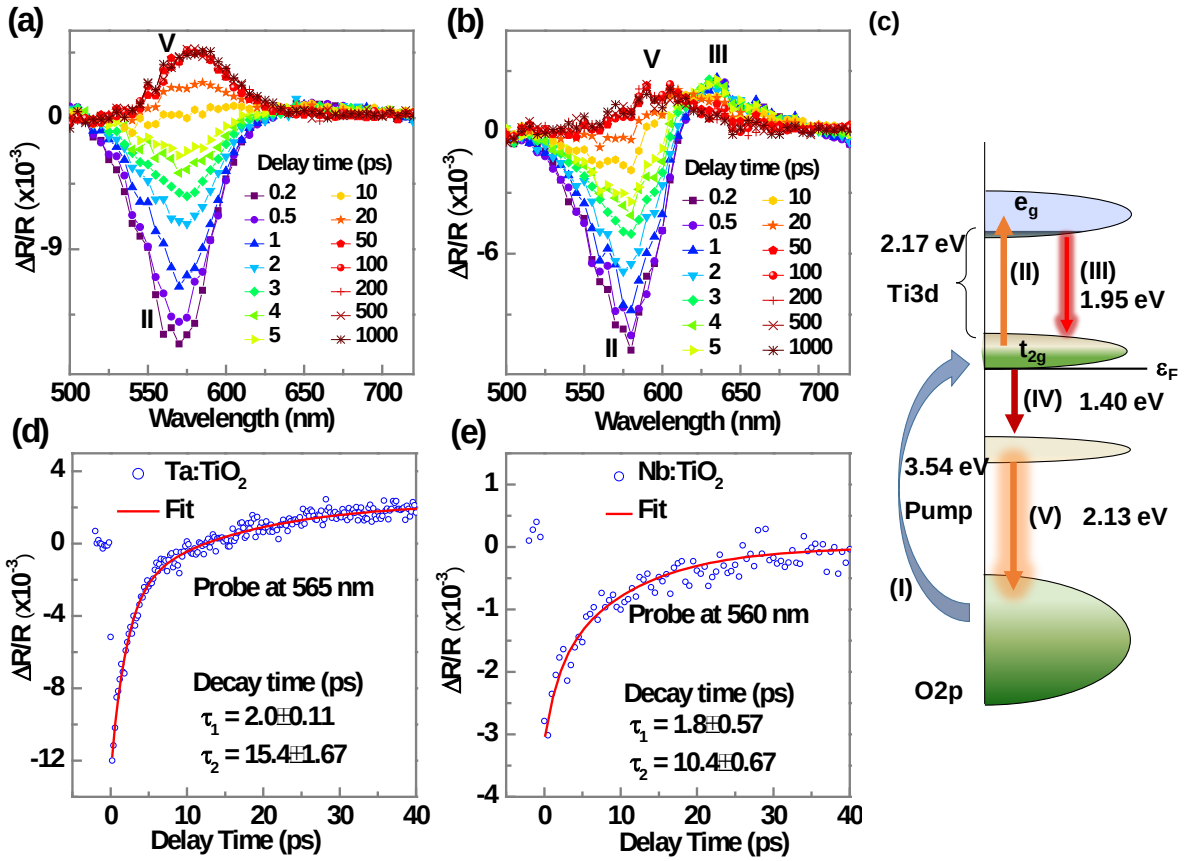

Fig. 2: Femtosecond transient absorption spectra of (a) Ta substituted TiO_2 and (b) Nb substituted TiO_2 thin films at different time delays with an excitation wavelength of 350 nm and energy density of 80 μJ/cm^2. (c) Schematic representation of the energy levels involved in the Femtosecond spectra. Kinetics of (d) Ta substituted TiO_2 and (e) Nb substituted TiO_2 thin films under an excitation wavelength of 350 nm and energy density of 80 μJ/cm^2.

Let us now look at the origin of small polaron, which is identified to be a result of the trapping of an electron with a cationic defect state in the system. In both Ta and Nb substituted TiO_2 cases, Ta and Nb act as donors by substituting Ti in the lattice which provides electrons to the conduction band. The increase in electron density will cause the system to compensate by either producing Ti^{3+} or Ti-vacancies. We demonstrate from ellipsometric measurements that the small polaron formation is a result of Ta and Nb substitution in TiO_2 which is absent in undoped TiO_2 and the mid-gap energy is a function of Ta/Nb concentration (Figure S8). To understand the presence of Ti^{3+}, XPS study has been carried out which is shown in Figure 3a-c. XPS data suggests that Ta is in the 5+ state whereas Nb exhibits mixed valence of 5+ and 4+ state. For a growth temperature of 600^{o}C and oxygen partial pressure of $1x10^{-4}$ Torr, majority of the Ti is in the 4+ state with a small percentage of Ti^{3+} in both Ta and Nb substituted TiO_2 samples. On a relative basis the Nb sample has close to double the number of Ti^{3+} defects compared to the Ta case. We speculate that in the case of $Ti_{0.94}Ta_{0.06}O_2$ there would be more Ti vacancies (V_{Ti}) as has been shown earlier in thin films of this composition to have exhibited ferromagnetism arising from V_{Ti}.[9] To confirm the presence of Ti-vacancies, we have performed XAS and the results are shown in Figure 3d for normal incidence configuration. Typically, XAS spectra provide information about unoccupied (empty) states. Metal L-edge absorption features probe the transition from 2p – 3d orbitals. The 2p spin-orbit coupling splits the initial state into $2p_{3/2}$ and $2p_{1/2}$, resulting in two L-edge features, denoted L_3 and L_2 respectively. As both the L_3 and L_2 edges arise from the transition to the 3d orbitals, they are affected by the ligand-field (crystal field) and multiplet effects, etc. causing further splitting of each edge to the characteristic t_{2g} and e_g levels. In our case, L_3-e_g feature splits into a doublet, reflecting slightly deformed symmetry of TiO_6^{8-}octhahedron, predicted by Jahn-Teller theory.[10] As can be seen in Figure 3d, the

spectral weight (intensity) for the $Ti_{0.94}Ta_{0.06}O_2$ is larger than for $Ti_{0.94}Nb_{0.06}O_2$. This is interpreted in terms of the increased concentration of V_{Ti} in the case of

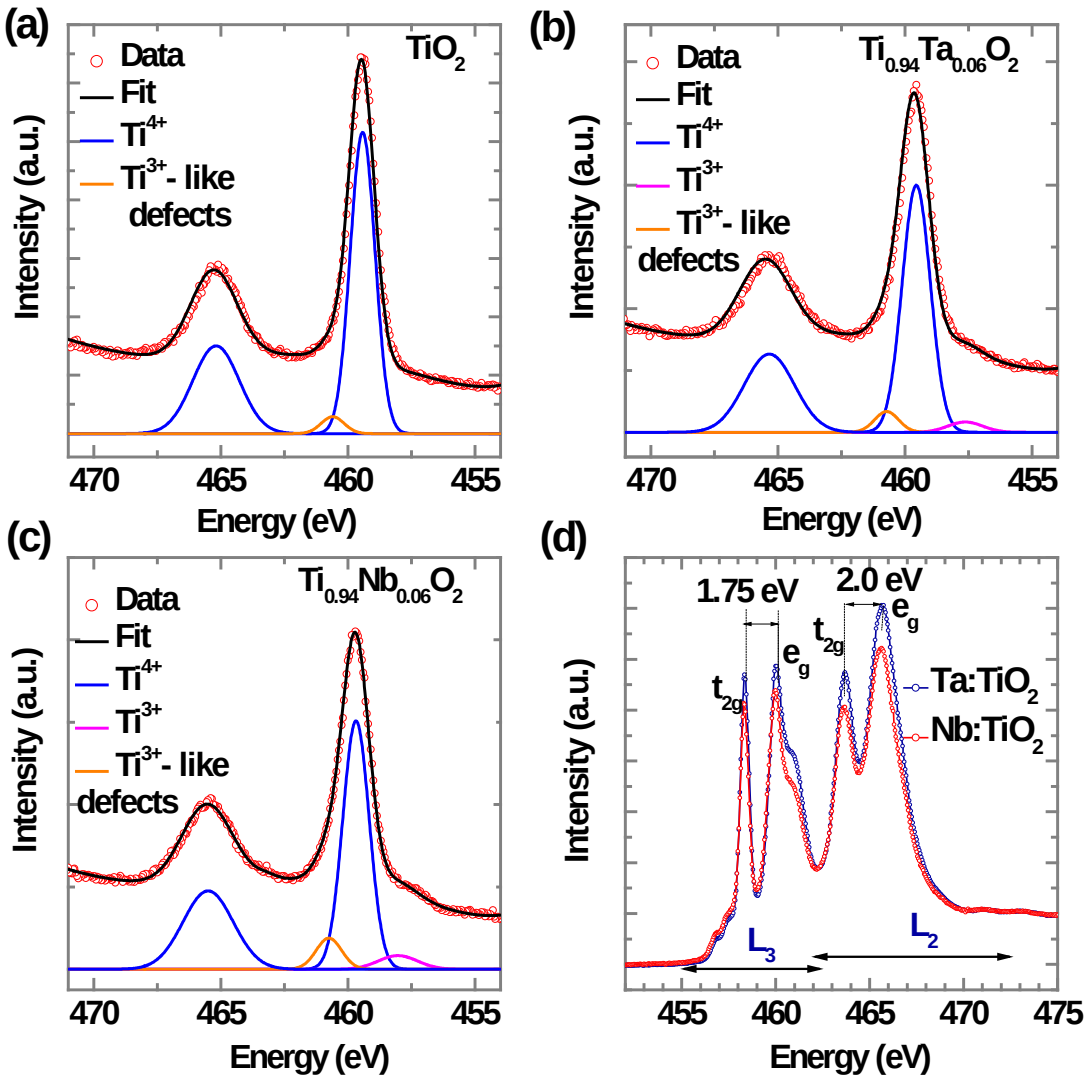

Fig. 3: X-ray photoelectron spectrum of (a) undoped TiO_2, (b) $Ti_{0.94}Ta_{0.06}O_2$ and (c) $Ti_{0.94}Nb_{0.06}O_2$ where all the samples are prepared at the same oxygen partial pressure of $1x10^{-4}$ Torr. Note the presence of Ti^{3+} in Nb and Ta substituted TiO_2 samples. However, it is either absent or weak in undoped TiO_2 sample. A Ti^{3+} like peak is seen in most of the samples with different fractions, it is mostly related to the presence of Ti_2O_3 like phases. (d) X-ray absorption spectra of $Ti_{0.94}Nb_{0.06}O_2$ (red, prepared at $PO_2=1x10^{-4}$ Torr) and $Ti_{0.94}Ta_{0.06}O_2$ (green, prepared at $PO_2=1x10^{-4}$ Torr). Note the presence of t_{2g} and e_g levels. The spectra are displayed after background subtraction followed by normalization.

Ta substituted TiO_2 sample on account of the observed increase in the density of final states. It is to be noted that the spectra have been subtracted for background at low and high energies (far from the absorption peaks). Any unoccupied Ti^{4+} will form four holes which will hybridize with oxygen orbitals; therefore Ti vacancies will essentially form states in the O_{2p} band. Four holes, created in the system as a result of V_{Ti} formation will increase the total number of 3d unoccupied states, and hence cause increased spectral weight, as can be seen in case of Ta samples relative to Nb ones.

Thus the XAS and XPS data bring out the subtle differences in the nature of the cationic defects in the Nb and Ta substituted TiO_2. The energy separation between the t_{2g} and the e_g measured by XAS is 1.71 eV which including the width of the bands would agree with the energy separation of 1.95 eV measured from the fs-TA. Further the differences in the mid gap states in the two cases is also consistent with the dominant nature of the defects, Ti^{3+} for Nb and V_{Ti} for Ta. The large mid gap state with a long time constant seen in the case of Ta must hence be attributed to deep levels associated with V_{Ti} as these levels are significantly reduced for the case of Nb. Hence the nature of the small polarons in the two cases is associated with two different cationic defects as well.

The evidence of both small and large polarons in doped TiO_2 with enhanced effective mass makes them a potential candidate for thermoelectric converters and the future studies could exploit this issue. Additionally, the rapid decay of the t_{2g} and e_g levels could be utilized for ultrafast optical switching.

Conclusions

Through a complementary approach of electrical transport and fs-TA, we provide strong experimental evidences for the presence of large and small polarons in epitaxial thin films of Ta and Nb substituted anatase TiO_2. The large polarons exhibit room temperature metallic conductivity with a T^3 dependence of the resistivity. The ionized impurity scattering

dominates at low temperatures due to a large concentration of ionized donors (Ta^{5+} and Nb^{5+}). fs-TA reveals the presence of small polarons which form mid-gap levels with a long carrier life time > 1 ns. XPS results indicate the presence of Ti^{3+} states which may be responsible for the small polarons. In addition, fs-TA provides evidence for the existence of excited states t_{2g} and e_g with a short carrier life time. XAS results further confirm the presence and separation of these levels which is a very important finding of this work.

References

1 Y. Ma, X. Wang, Y. Jia, X. Chen, H. Han and C. Li, *Chem. Rev.*, 2014, **114**, 9987.
2 B. J. Morgan, D. O. Scanlon and G. W. Watson, *J. Mater. Chem.*, 2009, **19**, 5175.
3 S. Moser, L. Moreschini, J. Jaćimović, O. S. Barišić, H. Berger, A. Magrez, Y. J. Chang, K. S. Kim, A. Bostwick, E. Rotenberg, L. Forró and M. Grioni, *Phys. Rev. Lett.*, 2013, **110**, 196403.
4 N. Serpone, *J. Phys. Chem. B*, 2006, **110**, 24287.
5 X. Chen, L. Liu, P. Y. Yu and S. S. Mao, *Science*, 2011, **331**, 746.
6 H. Ariga, T. Taniike, H. Morikawa, M. Tada, B. K. Min, K. Watanabe, Y. Matsumoto, S. Ikeda, K. Saiki and Y. Iwasawa, *J. Am. Chem. Soc.*, 2009, **131**, 14670.
7 T. Yamamoto and T. Ohno, *Phys. Rev. B*, 2012, **85**, 033104.
8 D. B. Poker and C. E. Klabunde, *Phys. Rev. B*, 1982, **26**, 7012.
9 A. Rusydi, S. Dhar, A. R. Barman, Ariando, D.-C. Qi, M. Motapothula, J. B. Yi, I. Santoso, Y. P. Feng, K. Yang, Y. Dai, N. L. Yakovlev, J. Ding, A. T. S. Wee, G. Neuber, M. B. H. Breese, M. Ruebhausen, H. Hilgenkamp and T. Venkatesan, *Phil. Trans. R. Soc. A*, 2012, **370**, 4927.
10 J. P. Crocombette and F. Jollet, *J. Phys. Condens. Matter*, 1994, **6**, 10811.

The table of contents entry

Substitution of Ti with Nb or Ta in epitaxial thin films of anatase TiO_2 induces large and small polarons.

ToC figure